Achieving Al Melt/Carbon and Al-Ti Melts/Carbon Interfaces Wetting *via* Ultrasonic Couple Processing

Y.L. LI and T.G. ZHOU

Good wetting among Al, Al-Ti melts and C (carbon) solid was achieved by ultrasonic couple processing (UCP). Due to the action of interfacial tension of wetting, Al melt and Al-Ti melts climb along the side wall of C solid. The wetting angle at the triple junction of gaseous, liquid, and solid phases is all lower than 15 deg. In the meantime, good wetting between Al melt and C powder was also achieved by the ultrasonic couple processing. Al melt infiltrated into the interior of C powder through the capillarity. When the ultrasonic couple processing was applied in the system of wetting between Al-Ti melts and C powder, owing to the superimposed effect of incident acoustic wave and reflected acoustic wave at Al-Ti melts/C interface, local high temperature occurred in the Al-Ti melts near C interface, and the superimposed effect can effectively obstruct a direct reaction of Al melt and C, inhibit the formation of undesirable Al_4C_3, and promote dissolved Ti to react with C and dissociated C to form TiC particle phase.

DOI: 10.1007/s11661-013-1667-1

I. INTRODUCTION

Al-Ti-C is a highly efficient grain refiner of aluminum and its alloys. Compared with Al-Ti-B, its nucleation particle phase TiC has smaller aggregation tendency than TiB_2, and Al-Ti-C also achieves good grain refinement in aluminum alloys containing Zr(<0.03 wt pct), Cr, and Mn elements. Therefore, Al-Ti-C, a substitute of Al-Ti-B grain refiner, is a new generation grain refiner.[1–3]

Integrating the high hardness, high elastic modulus, and excellent thermal stability of reinforced phase with the high ductility, good heat conductivity, and electrical conductivity of aluminum matrix, TiC particle-reinforced aluminum matrix composite possesses many advantages, such as high specific strength, abrasion resistance, and strong heat-transfer capability. In the meantime, TiC has good match of lattice structure with α-Al, which can nucleate directly on TiC particles, and hence, the compatibility of TiC/Al interface can be improved significantly.[4] TiC particle-reinforced aluminum matrix composite is a high performance structure material.[5]

However, because of the bad wettability between C and Al-Ti melts during the *in situ* synthesis of Al-Ti-C grain refiner and TiC particle-reinforced aluminum matrix composite,[6] C powder often absorbs impurity such as gas, is apt to produce hydrogen bond and agglomerate. Thus, Al melt is difficult to infiltrate into the interior of C powder to react with C. In the meantime, C powder is apt to float on the surface of Al-Ti melts, and oxidation reaction occurs when in contact with air. As the oxide film on the surface of Al-Ti melt also obstructs the wetting and reaction, a TiC synthesis reaction almost cannot occur between Al-Ti melts and C.

A high-density ultrasonic wave possesses an acoustic cavitation effect and acoustic streaming action.[7] It can change the mass transfer behavior of metallic melt and is used in the purifying, degassing, and microstructural refinement of the metallic melt.[6–10] It can also improve the wettability and nucleation capability between the reinforced phase and the metallic melt, and hence, it can improve the strengthening effect of particle phase. Furthermore, it can also have an influence on the migration and movement of the reinforced phase, make the reinforced particle phase gain external energy, release the agglomeration state from the clustering, and distribute dispersively. Thus, the acoustic cavitation effect and acoustic streaming action of ultrasonic wave are especially suitable for preparing a high-performance Al-Ti-C grain refiner and TiC particle-reinforced aluminum matrix composite.[11–14]

In the current work, ultrasonic couple processing (UCP) couples the ultrasonic wave to the vibration body, *i.e.*, graphite substrates, forms high-density acoustic field in Al melt and Al-Ti melts through optimizing the coordination condition of sound field, transfers the energy to the Al melt/C interface and Al-Ti melts/C interface through the propagation of sound field, and finally achieves the wetting at Al melt/C and Al-Ti melts/C interfaces under ultrasonic field. In the meantime, the cavitation effect leads to the occurrence of high-temperature thermal disturbance at TiC interface, stimulates the nucleation activity of refinement attenuated TiC particle phase, improves the compatibility of TiC/Al interface, obstructs the formation of Al_4C_3 due

Y.L. LI, Professor, is with the School of Materials and Metallurgy, Northeastern University, Shenyang 110004, P.R. China. Contact e-mail: liyl@smm.neu.edu.cn T.G. ZHOU, Professor, is with the School of Mechanical Engineering, Shengyang University, Shengyang 110044, P.R. China.

Manuscript submitted November 2, 2012.
Article published online March 6, 2013

to the direct reaction of Al melt and C, and promotes the synthesis reaction of TiC.

II. EXPERIMENTAL

The experimental alloys were pure aluminum A1075 and Al-3Ti, Al-5Ti, and Al-10Ti alloys (in wt pct), in which Al-Ti alloys was prepared by liquid–solid reaction. The raw materials used for liquid–solid reaction were K_2TiF_6 (≥99.8 wt pct) and pure aluminum A1075. Its reaction temperature was 1033 K (760 °C) and its reaction time was 30 minutes.

There were two kinds of C substrates: One was made of high-purity graphite solid, which was fabricated into a crucible shape and a plane shape. The other one was made by hot-pressed high-purity graphite powder, which was fabricated into a plane shape. The density of this substrate was about 90 pct of the density of graphite solid. The aforementioned two kinds of substrates all passed mechanical polishing with diamond pastes, and the average surface roughness Ra was <0.01 μm for the former and <0.05 μm for the latter.

The wettability measuring system with ultrasonic field coupling device was shown in Figure 1.

The system consisted of a vacuum chamber, a heating chamber (in which ring Ta heating element and Mo baffle board was mounted), a vacuum system containing a diffusion pump and a molecular pump (the content of oxygen was reduced as far as possible through the molecular sieve and oxygen trap), a melt addition tube and a rotary objective table, a temperature-controlling device, an ultrasonic field-coupling device (including the ultrasonic generator, the power regulator and the transducer, the work mode of in which the generator was separate excitation, its final stage used the power module switching power supply type power amplifier, its predictor control adopted analog type and pulse width modulation (PWM) mode, and frequency, pulse width and power were adjustable continuously), a set of 10-mW laser source with the wave length of 632.8 nm, a special filter (filtering off entire other wave length rays other than the laser beam with the wave length of 632.8 nm), a high-definition digital camera in 2000 × 1312 pixels, and a computer.

High-definition molten drop backlight photographs were obtained by this system. The curve equation about the molten drop contour was obtained by curve fitting. The wetting angles and contact radii were analyzed and calculated, the wetting characteristics were analyzed, and the effects of ultrasonic couple parameters, temperature, time, and substrate characteristics on the interfacial wetting were investigated. A scanning electron microscope (SEM) and electron microprobe energy dispersive spectrometer (EDS) were used for the observation of interfacial microstructures and the analyses of the distribution of alloy elements. The wetting behavior among Al, Al-Ti melts, and C, as well as the reaction mechanism, were investigated.

The experimental alloys were melted in another electric resistance furnace to 973 K (700 °C) for 20 minutes holding. One took out 3-g metallic melts and poured it into the melt addition tube. The melts passed the melt addition tube and flowed onto the C substrate to form a molten drop. Then the upper end of the melt addition tube was closed down. The vacuum chamber was vacuumized. When the degree of vacuum reached 10^{-4} Pa, the temperature in the heating chamber was set to a certain value in the temperature range from 973 K to 1423 K (700 °C to 1150 °C). The variations in the

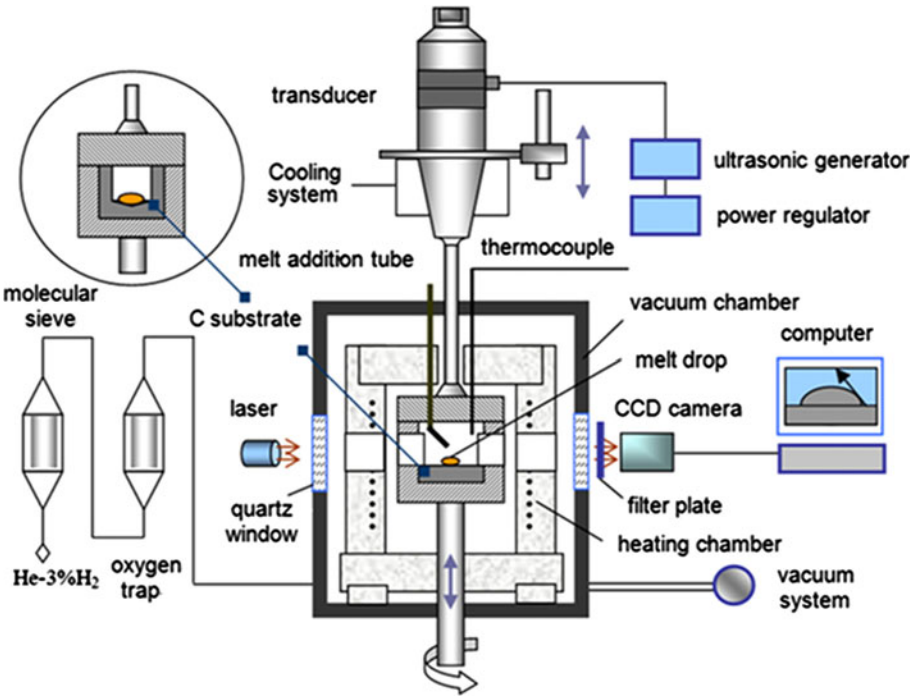

Fig. 1—UCP wettability measuring system.

wetting status at Al melt/C and Al-Ti melts/C interfaces with temperature and time were recorded by the wettability measuring system. The wetting kinetic curves were obtained after one processes the gathered experimental data through the computer. Its ultrasonic frequency was 20 KH_Z, pulse width was 25 μs, and power was 50 W. When the experiment was finished, *i.e.*, the shape of molten drop reached an equilibrium state, the heating system was closed down. The pressure in the vacuum chamber recovered to the normal atmospheric pressure. The experimental alloy cooled and solidified after one blew in argon gas. The wetting couple samples of Al melt/C interface and Al-Ti melts/C interface were obtained. Then the samples were cut open along their longitudinal directions and ground by abrasive papers and polished. Macroscopic photographs were taken by the digital camera. After the polished samples were etched in the dilute hydrofluoric acid aqueous, the microstructure observation and analyses were conducted on SEM and electron microprobe EDS.

III. RESULTS AND DISCUSSION

A. *Effect of UCP on the Wetting Among Al, Al-Ti Melts and C Solid*

The wetting status among Al, Al-3Ti, Al-5Ti, and Al-10Ti melts and C solid at the temperatures of 993 K, 1033 K, 1073 K, and 1103 K (720 °C, 760 °C, 800 °C, and 830 °C) for 60 min holding without UCP is shown in Figure 2. The C solid is high-density, high-purity graphite that is fabricated into a crucible shape. The bottom of the crucible is drilled with a cone angle of 120 deg so as to reduce as far as possible the effect of self-weight of molten drop on the shape of molten drop.

It is found from Figure 2 that the effect of temperature and Ti content on the shapes of molten drop varies little; the aluminum molten drop basically takes on sphericity, and the wetting angle between the melts and C is all greater than 150 deg. These results show that at these experimental temperatures, wetting does not exist among Al, 3Ti, Al-5Ti, and Al-10Ti melts and C solid.

The wetting status among Al, Al-3Ti, Al-5Ti, and Al-10Ti melts and C solid at the temperatures of 993 K, 1033 K, 1073 K, and 1103 K (720 °C, 760 °C, 800 °C, and 830 °C), respectively, for a holding time of 30 minutes in the heating chamber with UCP is shown in Figure 3.

As shown in Figure 3, UCP significantly improves the wettability among Al, Al-Ti melts and C interfaces so that Al melt and Al-Ti melts spread along the bottom of graphite crucible and climb upward along the sidewall of the crucible. In the meantime, the effect of temperature and alloy composition on the state of wetting does not differ obviously. The wetting angles in the stable state at the junction of the melt, gaseous phase, and C solid phase interfaces obtained in Figure 3 are shown in Table I.

Electron microprobe EDS analyses show that interfacial reaction does not occur among Al, Al-Ti melts and C interfaces in Figure 2, *viz.*, Al_4C_3 and TiC intermetallic compound does not form. A reaction also does not occur between Al melt and C interface in Figure 3(a), *viz.*, Al_4C_3 intermetallic compound does not form. On the contrary, reaction occurs between Al-Ti melts and C interface in Figures 3(b) through (d), and TiC intermetallic compound forms but Al_4C_3 intermetallic compound does not form.

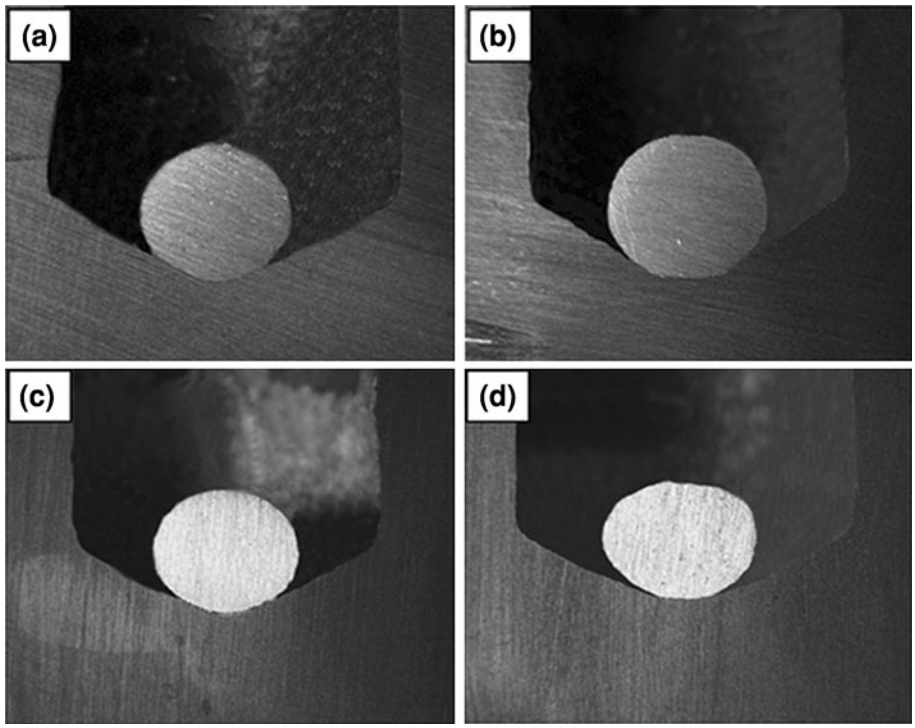

Fig. 2—The macrophotographs showing wetting status among Al, Al-Ti melts and C solid without UCP: (*a*) 993 K (720 °C)-(Al), (*b*) 1033 K (760 °C)-(Al-3Ti), (*c*) 1073 K (800 °C)-(Al-5Ti), and (*d*) 1103 K (830 °C)-(Al-10Ti).

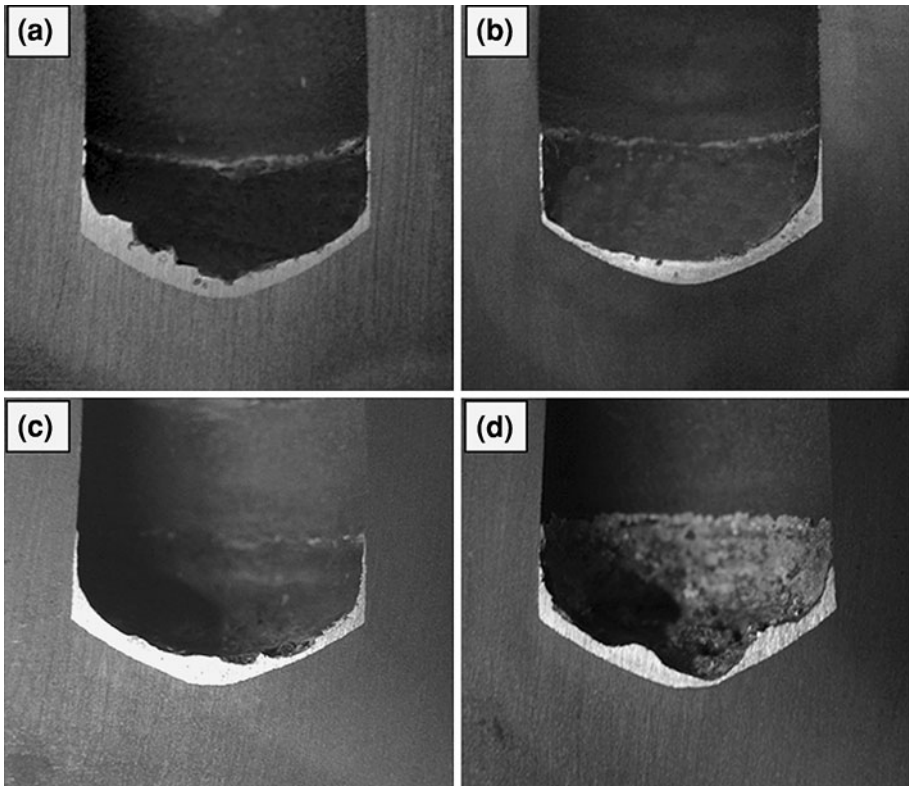

Fig. 3—The macrophotographs showing wetting status among Al, Al-Ti melts and C solid with UCP: (*a*) 993 K (720 °C)-(Al), (*b*) 1033 K (760 °C)-(Al-3Ti), (*c*) 1073 K (800 °C)-(Al-5Ti), and (*d*) 1103 K (830 °C)-(Al-10Ti).

Table I. Measuring Results of Wetting Angle in Stable State Using Wetting Couple in Fig. 3

Type of Wetting Couple	(a) -(Al)	(b) -(Al-3Ti)	(c) -(Al-5Ti)	(d) -(Al-10Ti)
Wetting angle in steady state (deg)	5	7	10	15

B. *Effect of UCP on the Wetting Among Al, Al-Ti Melts and C Powder*

The wetting status among Al, Al-Ti melts and C powder with UCP is shown in Figure 4.

It is noted in Figures 4(a) and (b) that under the action of wetting interfacial tension, Al melt and Al-Ti melts can infiltrate into the interior of C powder through capillarity. In the meantime, the Al-Ti melts infiltrated into the interior of the C powder have reacted with the C powder. A large number of TiC particle phases has formed and their morphology takes on clustering distribution. Moreover, a rich Ti layer exists at the boundary of C powder, indicating that Ti atoms in the melt have diffused to the periphery of the C powder, which provides a good interfacial condition for the synthesis reaction of TiC. However, Al_4C_3 intermetallic compound does not appear in the reaction between Al-Ti melts and C powder.

According to the thermodynamics condition, the reaction formula and variation in Gibbs free energy for graphite (C) to become dissociated graphite ($\underline{C}$) atoms (the unit of $\triangle G$: KJ/mol) are as follows[14]:

$$C(S) \rightarrow \underline{C} \quad [1]$$

$$\Delta G_1^o = 71431 - 45.970T \quad [2]$$

It can be observed from Eq. [2] that when reaction temperature is higher than 1553 K (1280 °C), ΔG_1^o is a negative value, and reaction [1] can occur according to thermodynamical law, *i.e.*, C can become dissociated $\underline{C}$ atoms in Al melt.

The reaction formula of Al_4C_3 formed by the reaction of C and Al melt and Gibbs free-energy formula (the unit of $\triangle G$: KJ/mol) are as follows[15]:

$$\underline{C} + Al(l) = Al_4C_3 \quad [3]$$

$$\Delta G_2^o = -89611 + 32.841T \quad [4]$$

$$C(s) + Al(l) = Al_4C_3 \quad [5]$$

$$\Delta G_3^o = -161042 + 78.811T \quad [6]$$

It can be seen from Eqs. [4] and [6] that when the reaction temperature is higher than 2728 K (2455 °C), ΔG is a positive value, and reactions [3] and [5] cannot occur according to thermodynamical law; *i.e.*, Al_4C_3

hazardous compound does not form when Al melt and C have wetted. These analyzing results have been proved by Figures 3 and 4.

With UCP, the incident acoustic wave and reflected acoustic wave at the Al melt/C interface possess a superimposed effect because acoustic resistance Z_C is greater than Z_{Al} and the transmission coefficient of acoustic pressure for graphite $D = 2Z_C/Z_C + Z_{Al}) > 1$. The C interface has an acoustic pressure amplification influence on the transmission acoustic wave. Air bubbles collapse within an extremely short time. This process is equivalent to an adiabatic process. When pressure is imposed due to the collapse of air bubble, the temperature at the C interface rises. Hot stream flows from the pressed side to the unpressed side, absorbs the energy caused by the collapse of air bubble, and changes the energy into heat energy. The result is a local high temperature in the melt adjacent to the Al melt/C interface. Thus, local high temperature causes C to become dissociated C atoms in Al melt. In the meantime, a high-temperature condition can effectively obstruct the formation of Al_4C_3 due to the direct reaction of Al melt with C and C. Here, TiC is formed in following reactions, *i.e.*,

$$\underline{Ti}C(s) = TiC \quad [7]$$

$$\underline{Ti} + \underline{C} = TiC \quad [8]$$

Therefore, UCP promotes the formation of dissociated C atoms, obstructs the formation of Al_4C_3, alters the path of forming TiC, raises its reaction activity, and promotes the synthesis reaction of TiC.

C. *Wetting Kinetic Curve Among Al, Al-Ti Melts and C Solid Under UCP*

The variation in wetting angle of Al melt and Al-Ti melts on the plane shape substrates of C solid with time and temperature in the temperature range from 993 K to 1423 K (720 °C to 1150 °C) with UCP is shown in Figure 5.

The variation in wetting angle of Al melt and Al-Ti melts on the substrates of C solid with time is shown in Figure 5(a).

It is shown that under UCP, the wetting process at Al melt/C interface and Al-Ti melts/C interface can be divided into two stages: quasi-stable-state decrease stage and tending-to-be-stable stage. There is no incubation stage occurring during conventional wetting process. The wetting angle varies greatly within 10 minutes prior to the holding. Moreover, the influence of temperature and Ti content on the time, t_0 (about 35 minutes), when contact angle in stable state is attained, is rather small. In the meantime, although TiC (Figures 3(b) through (d)) forms due to the interfacial reaction at Al-Ti melts/C interface, *viz.*, reaction wetting occurs, the quasi-stable-state contact angle at Al-Ti melts/C interface is still less than that at Al melt/C interface because the surface tension of Al-Ti melt at 1123 K (850 °C) is less than that of Al melt at 993 K (720 °C). Al-Ti melt is more apt to spread along the C interface, and hence, its wetting angle is relatively small.

The variation in wetting angle of Al melt and Al-Ti melts on the substrates of C solid with temperature is shown in Figure 5(b). It can be seen from curves 2 and 3 that under UCP, although the wetting angle takes on a decreasing trend with increasing temperature, the change in temperature does not have an obvious influence on the contact angle in the stable state. Furthermore, the wetting angle of Al-Ti melts and C at the same temperature is slightly greater than that of Al melt and C because the surface tension of Al-Ti melt is more than that of Al melt at the same temperature. Relatively speaking, Al melt is more apt to spread along the C interface, and hence, its wetting angle is relatively small.

According to the research results (see curve 1 in Figure 5(b)) from Eustathopoulos *et al.*,[6] without UCP, the wetting process of Al melt and C can be divided into three stages. The first stage is in the temperature range from 973 K to 1173 K (700 °C to 900 °C). The wetting angle takes on larger obtuse angle. The degree of decrease in the wetting angle is very small with the variation in temperature. The second stage is in

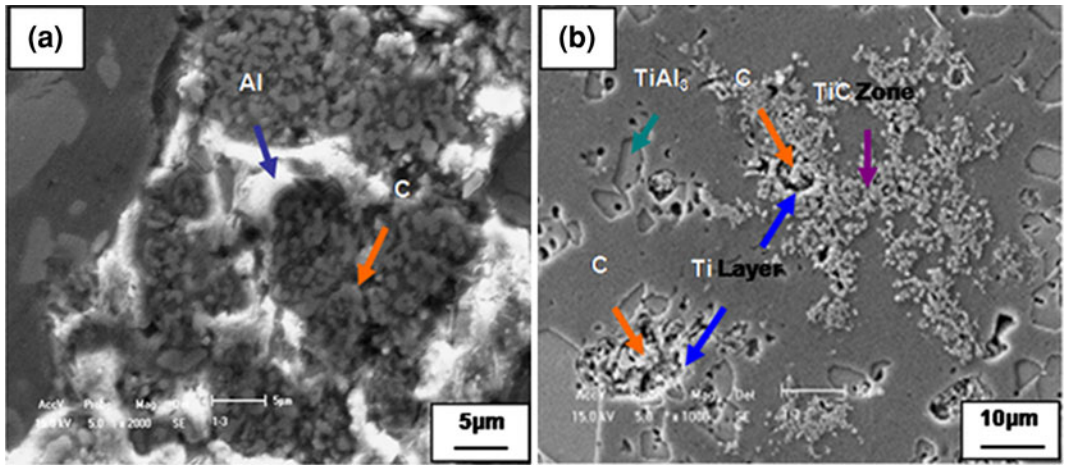

Fig. 4—Effect of UCP on the wetting among Al, Al-Ti melts and C powder: (*a*) Al/C powder and (*b*) Al-5Ti/C powder.

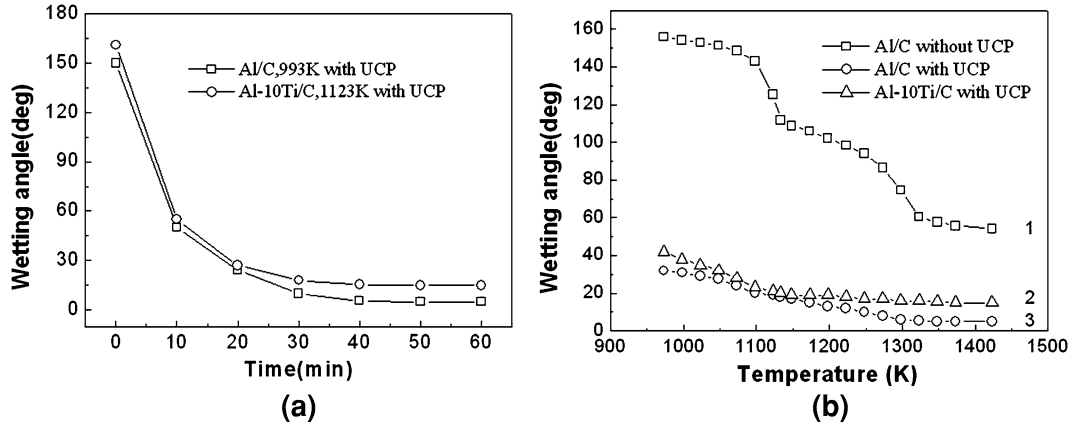

Fig. 5—Variation in wetting angle at Al melt/C solid and Al-Ti melts/C solid interfaces with time and temperature: (*a*) effect of time on the wetting angle and (*b*) effect of temperature on the wetting angle.

the temperature range from 1173 K to 1273 K (900 °C to 1000 °C). The wetting angle decreases greatly with increasing temperature. The third stage is in the temperature range more than 1273 K (1000 °C). At this point, the wetting angle is less than 90 deg, indicating that the wetting between Al melt and C has been achieved.

D. *Analysis of the Wetting Mechanism Among Al, Al-Ti Melts and C Solid Under UCP*

Comparing the results in the current work and those reported by Eustathopoulos *et al.*,[6] we propose following analysis of wetting mechanism among Al, Al-Ti melts and C solid.

It can be seen from Eq. [6] that when temperature is lower than 2043 K (1770 °C), ΔG is negative and reaction [5] can occur according to thermodynamical law. However, even under a vacuum condition, a layer of oxide film always exists on the surfaces of Al melt and Al-Ti melts. The oxide film obstructs direct contact of liquid–solid phase and hence Reaction [5] cannot proceed. That is to say, when the temperature is low (less than 1173 K [900 °C]), nonreaction wetting and reaction wetting phenomena cannot occur at the Al melt/C interface (see the first stage of curve 1 in Figure 5(b)). In the meantime, owing to the action of high surface tension on the oxide film, the shape of the molten drop is difficult to change. Thus, the phenomenon that the molten drop in Figure 2 takes on sphericity appears when UCP is not applied.

When the temperature is raised to the temperature range from 1173 K to 1273 K, the cracking and disappearance of oxide film on the surface of the molten drop can be observed. The reason is that at this point, a transformation of crystal structure occurs in the alumina thin film, the solubility of aluminum melt increases suddenly, and the gasification reaction $4Al + Al_2O_3 = 3Al_2O$(gaseous state) occurs.[16] In the meantime, when the expansion coefficient of aluminum is obviously greater than that of the oxide film, the cracking of the oxide film also occurs. As a result, reaction wetting occurs at the Al melt/C interface. Therefore, the phenomenon that rapid decrease of the wetting angle in the second stage of curve 1 in Figure 5(b) appears when UCP is not applied under this temperature condition.

When the temperature is in the temperature range from 1273 K to 1423 K (1000 °C to 1150 °C), the surface tension of Al melt decreases with increasing temperature. However, in this case, Al melt has wetted mutually with C and the wetting angle no longer decreases. Therefore, the phenomenon that slow decrease of the wetting angle in the third stage of curve 1 in Figure 5(b) appears when UCP is not applied under this temperature condition.

Nevertheless, when UCP is applied, on account of the acoustic cavitation effect and acoustic streaming action, the oxide films of Al melt and Al-Ti melts crack. At the same time, because the incident acoustic wave and reflected acoustic wave among Al, Al-Ti melts and C interface possess a superimposed effect, the cavitation phenomenon appears and high temperature occurs at the liquid–solid interfaces,[13] which improves the nonreaction wetting performance and results in reaction wetting (Reactions [7] and [8]). Therefore, the temperature condition of the melt has no obvious influence on practical wetting performance (Figure 5(b)) when UCP is applied.

In the meantime, when UCP is applied, besides enhancing the nonreaction wetting performance and raising the activity of interfacial reaction, the acoustic streaming action causes the interfacial reaction product TiC to mass transfer in good time to the melt and hence causes the wetting interface to achieve real-time renewal. Otherwise, the interfacial reaction product TiC particle phase will take on an agglomeration distribution morphology on the wetting interface, which will become a barrier against the wetting among Al, Al-Ti melts and the C interface. Therefore, the movement of the TiC particle formed by the reaction at the C interface is an importance influencing factor for achieving continuous wetting.

IV. CONCLUSIONS

A method of improving the wettability at Al melt/C and Al-Ti melts/C interfaces using a novel and efficient

ultrasonic couple processing was proposed. Good wetting among Al melt, C solid, and C powder was achieved using ultrasonic couple processing, and this wetting belongs to nonreaction-type wetting, whereas good wettability between Al-Ti melts and C resulted from nonreaction-type wetting and reaction wetting. At the same time, the renewal of wetting interface due to acoustic streaming action was the first cause for the wetting process to proceed continuously and stably when the ultrasonic couple processing was applied. Also, owing to the superimposed effect of incident acoustic wave and reflected acoustic wave at Al-Ti melts/C interface, local high temperature occurred in the melt adjacent to Al melt/C and Al-Ti melts/C interfaces, and the superimposed effect can effectively obstruct the formation of Al_4C_3 caused by the direct reaction of Al melt and C, promote dissolved Ti to react with C, and dissociate C to form TiC particle phase.

ACKNOWLEDGMENTS

This work was supported by the National Natural Science Foundation of China No. 51174061.

REFERENCES

1. D. Qiu, J.A. Taylor, and M.X. Zhang: *Mater. Sci. Eng.*, 2010, vol. A41, pp. 3412–21.
2. L. Yu, X.F. Liu, Z.Q. Wang, and X.F. Bian: *J. Mater. Sci.*, 2005, vol. 40, pp. 3865–67.
3. P. Moldovan and G. Popescu: *Alum. Alloy*, 2004, vol. 12, pp. 59–61.
4. X.W. Zeng, W.G. Zhang, N. Wei, and R.P. Liu: *Mater. Sci. Eng.*, 2007, vol. A443, pp. 224–28.
5. B. Ranjit: *Trans. Indian. Inst. Met.*, 2009, vol. 62, pp. 391–95.
6. N. Eustathopoulos, J.C. Joud, P. Desre, and J.M. Hicter: *J. Mater. Sci.*, 1974, vol. 9, pp. 1233–42.
7. G.I. Eskin: *Adv. Perform. Mater.*, 1997, vol. 4, pp. 223–32.
8. G.I. Eskin: *Metallurgist*, 2010, vol. 54, pp. 319–25.
9. X.B. Han, Y.H. Qing, and T. Thomas: *Mater. Sci. Eng. A*, 2008, vol. 473, pp. 96–104.
10. L. Zhang, G.I. Eskin, and L. Katgerman: *J. Mater. Sci.*, 2011, vol. 46, pp. 5252–59.
11. Y.L. Li, F.R. Cao, Y.B. Chen, and H.K. Feng: *Metall. Mater. Trans. A*, 2009, vol. 40A, pp. 2178–83.
12. Y.L. Li, H.K. Feng, F.R. Cao, and Y.B. Chen: *Wuhan Univ. Technol.-Mater. Sci. Ed.*, 2008, vol. 3, pp. 319–22.
13. Y.L. Li, H.K. Feng, F.R. Cao, and Y.L. Gong: *Mater. Sci. Eng. A*, 2008, vol. 487, pp. 518–23.
14. Z.W. Xua, L. Ma, J. Yana, S. Yanga, and S. Dub: *Compos. Part A*, 2012, vol. 43, pp. 407–14.
15. A.R. Roberta and X.J. Zhang: *Metall. Trans. A*, 1991, vol. 2A, pp. 3071–75.
16. V. Laurent, D. Chatain, C. Chatillon, and N. Eustathopoulos: *Acta Metall.*, 1988, vol. 36, pp. 1797–1803.